

## THE ROLE OF STRUCTURAL AND CHEMICAL PROPERTIES IN *pm-Si:H* THIN FILMS TO DETERMINE THE OPTOELECTRONIC CHARACTERISTICS AND STABILITY BY SOAKING LIGHT FOR APPLICATIONS IN SOLAR CELL.

C. Álvarez-Macías<sup>\*1</sup>, E. Barrera Calva<sup>1</sup>, F. González García<sup>1</sup>, L. Gómez<sup>2</sup> and G. Santana<sup>2</sup>.

<sup>1</sup>Universidad Autónoma Metropolitana-Iztapalapa, Área de Ingeniería en Recursos Energéticos. San Rafael Atlixco 186, Col. Vicentina, AP 55-534 C.P. 09340. México, D.F.

<sup>2</sup>Instituto de Investigaciones en Materiales, Universidad Nacional Autónoma de México. A.P. 70-360, Coyoacán, C.P. 04510, México, D.F.

\* Corresponding author: Carlos Álvarez Macías. Address: Unidad de Ciencias Básicas e Ingeniería, Departamento de Ingeniería de Procesos e Hidráulica, área de Ingeniería en Recursos Energéticos. Universidad Autónoma Metropolitana-Iztapalapa, San Rafael Atlixco 186, Col. Vicentina, AP 55-534. México, D.F. C.P. 09340. Tel: +52(55) 58 04 40 00 Ext (1236), Fax +52(55) 58 04 46 66.

e-mail: [alvarez.krlos@gmail.com](mailto:alvarez.krlos@gmail.com).

### Abstract

We examine the role of structural and chemical properties of Hydrogenated polymorphous Silicon, *Pm-Si:H*, thin films on the optoelectronic characteristics and the level of stability under prolonged white light exposure at 100 mw/cm<sup>2</sup> (AM1.5 condition), for applications in solar cells. These thin films were grown by Plasma Enhance Chemical Vapor Deposition (PECVD) using dichlorosilane (SiH<sub>2</sub>Cl<sub>2</sub>), instead of silane (SiH<sub>4</sub>) as precursor gas, at different hydrogen dilutions (*D<sub>H</sub>*). The nano-structural properties were confirmed by Raman measurements. The films compositions were determined by XPS measurements. From FTIR analysis we notice bonding configurations associated to photo-stability. Light soaking experiments during 250h show important behaviors on the electronic transport properties measurements to different levels of incorporated oxygen.

*Keywords: Polymorphous Silicon, Solar Cell, Photoconductivity.*

### 1. Introduction.

During the last decades extensive efforts have been made to overcome the light-induced degradation in amorphous silicon films. Currently huge interest has been drawn towards the use of nanocrystalline silicon as the intrinsic layer of a solar cell. At the same time, numerous works have been carried out to clarify the growth mechanism of amorphous, microcrystalline and polycrystalline silicon (a-Si:H, mc-Si:H and poly-Si) thin films [1]. Plasma-enhanced chemical vapor deposition (PECVD) using highly diluted silane (as precursor gas) in hydrogen mixtures allows the production of a wide range of silicon thin films with varying degrees of disorder [2]–[4]. The optimization of plasma conditions used for the growth of amorphous and microcrystalline silicon thin films has led to obtain different silicon crystalline phases (nanocrystals, microcrystals, etc.) embedded in an hydrogenated amorphous silicon, material called Hydrogenated polymorphous silicon (pm-Si:H) [4], [5]. Due to its specific nanostructure pm-Si:H is a suitable candidate for application in silicon-based thin film solar cells because, despite being heterogeneous, it exhibits improved electronic transport and stability properties after light-soaking compared to those of a-Si:H [4]. Normally, pm-Si films have been deposited by PECVD using highly diluted silane in hydrogen mixtures. However, the use of high hydrogen dilutions can contribute to an excessive incorporation of weak Si–H bonds into the pm-Si:H, obtaining in light-induced degradation of efficiency due to the so called Staebler–Wronski effect, resulting unsuitable for thin-film photovoltaic applications [6]. Alternative passivating atoms with higher mass and lower diffusion coefficient than hydrogen, such as chlorine, are being investigated. Consequently, Chlorinated silanes, i.e., SiH<sub>2</sub>Cl<sub>2</sub>, SiHCl<sub>3</sub> and SiCl<sub>4</sub> have been used aiming at the improvement of material properties [1]. The use of chlorine in PECVD processes

has shows, i) increases crystallization process, ii) pos thermal annealing are no necessities and iii) minor incorporation of weak Si-H bonds [4]. Recently, using dichlorosilane ( $\text{SiH}_2\text{Cl}_2$ ) we have obtained different crystalline silicon formations (nc-Si to  $\mu\text{c-Si}$ ) inside of the amorphous matrix, depending on the deposition conditions [3], [7], [8]. However, more extensive studies about the effects of chlorine chemistry in plasma systems are needed. In this work we had examined the role of structural and chemical properties of material to determine the optoelectronic characteristics of the material and, therefore, the level of stability under prolonged light exposure. We analyze the correlations between photoconductivity measurements and chemical composition, oxidation level, crystalline volume fractions, mean grain size and optical band gap.

## 2. Experimental.

Pm-Si thin films were grown in a conventional PECVD system with parallel plates of  $150\text{ cm}^2$  and  $1.5\text{ cm}$  apart, activated by a RF signal of  $13.56\text{ MHz}$ . Depositions were performed at pressures of  $250$  and  $500\text{ mTorr}$  and hydrogen dilutions ratio,  $R_H = \text{H}_2/(\text{SiH}_2\text{Cl}_2+\text{H}_2)$ , of  $83.3$ ,  $90.9$ ,  $93.8$  and  $95.2$ , keeping the other deposition parameters constant. Growth conditions are summarized in Table 1. Nano-structural analysis was performed using a Raman equipment model T64000 with Horiba Jobin-Yvon triple monochromator. The excitation source was an Ar+ Lexcel laser of  $514.5\text{ nm}$ . All measurements were performed at room temperature in air. The samples were irradiated at a power of  $20\text{ mW}$  in a spot size around  $1\text{ mm}^2$  to prevent laser-induced crystallization. The measuring range was between  $400$  and  $600\text{ cm}^{-1}$ , the integration time of measurements was  $1\text{ min}$  and the Raman signal was acquired by a cooled CCD detector. The atomic compositions were obtained by X-ray Photoelectron Spectroscopy (XPS) analysis in a VG Microtech Multilab ESCA 2000 system, equipped with a hemispherical-multichannel detector CLAM4-MDC, in which we determined the presence of Cl and O in the samples. Fourier transform infrared (FTIR) spectra of the films were recorded in absorbance mode using a Nicolet-210 FTIR spectrometer in the range  $400\text{--}4000\text{ cm}^{-1}$  on thin-film samples deposited on polished crystalline silicon substrates. Optical properties were investigated by means of optical band gap, which was deduced from the absorption spectrum between  $1$  and  $3.0\text{ eV}$  by a JASCO V630 spectrometer UV-VIS, using the Tauc Model, where the films thicknesses were obtained by typical profilometry. Variation of photoconductivity of all these films was investigated under a light intensity of  $100\text{ mW/cm}^2$  for  $250\text{ h}$  of light soaking by measuring the current and voltage. The light soaking treatment was realized in homemade equipment under AM 1.5 spectrum and the temperature was controlled at  $25^\circ\text{C}$  by heat dissipation.

## 3. Results and discussion.

### 3.1. STRUCTURAL PROPERTIES BY RAMAN.

Each spectrum obtained by Raman measurements was deconvoluted at the best fit corresponding to amorphous, nanocrystalline and microcrystalline phases [4], [9]. The peaks of the amorphous and microcrystalline phases are fixed at  $480\text{ cm}^{-1}$  and  $520\text{ cm}^{-1}$ , respectively [3], [10]–[12]. The third peak, associated to the nanocrystalline phase, is located at the best fit between  $500$  and  $519\text{ cm}^{-1}$  [4], [12]. Each spectrum was deconvoluted following the next criteria: two Lorentzian curves, corresponding to nano and microcrystalline contributions, and a Gaussian curve corresponding to the amorphous phase [4]. We obtained the crystalline volume fraction,  $X_C$ , using relation 1 [4], [11], [13]. The area of the curves are designated as  $I_A$ ,  $I_N$ , and  $I_C$ , for the peaks of amorphous, nanocrystalline and microcrystalline phases, respectively.

$$X_C = \frac{I_N + I_C}{I_N + I_C + I_A} \quad (\text{eq.1})$$

while the mean grain size,  $D_R$ , is calculated using relation 2 which is based on the quantum confinement model where  $\Delta\nu$  is the frequency peak shift of the nanocrystalline phase with respect to  $520\text{ cm}^{-1}$  [4], [11]. At the same table 1, values of both properties are also presented.

$$D_R = 2\pi\sqrt{2.24/\Delta\nu} \quad (\text{eq.2})$$

Table 1 shows results of both  $X_C$  and  $D_R$ , as a function of dilution of hydrogen for both pressures. To detect the behavior of these parameters with better accuracy, the uncertainty of each data using standard deviation of three different deconvoluciones made to each spectrum was obtained.

**Table 1. Growth conditions of pm-Si:H thin films deposited by PECVD, structural and optoelectronic Results as a function of dilution of hydrogen for both pressures.**

RF Power = 150 W, flows: Ar = 50 sccm and SiH <sub>2</sub> Cl <sub>2</sub> = 5 sccm. T <sub>substrato</sub> = 200°C. Time of Growth 30 min			Structural Parameters		Effective Optical Band Gap	Photoconductivity % Degradation or improvement
Dilution D <sub>H</sub> [%]	Thickness [nm]	Growth rate (nm/min)	X <sub>C</sub> [%]	D <sub>R</sub> [nm]	[eV]	$\left(\frac{\sigma_2 - \sigma_1}{\sigma_1}\right)$
Pressure of 250 mTorr						
83.3	268	9.1	70 ± 18	2.7 ± 0.3	1.75 ± 0.09	34%
90.9	291	10.8	83 ± 14	2.4 ± 0.2	1.66 ± 0.09	34%
93.8	235	10.1	69 ± 7	3.2 ± 0.5	1.36 ± 0.03	-15%
95.2	284	11.8	94 ± 15	4.2 ± 0.4	1.18 ± 0.09	-68%
Pressure of 500 mTorr						
83.3	214	7.8	92 ± 12	2.8 ± 0.3	1.75 ± 0.04	65%
90.9	223	8.2	65 ± 16	3.1 ± 0.3	2.12 ± 0.03	-92%
93.8	245	9.4	95 ± 19	3.3 ± 0.2	1.15 ± 0.06	-191%
95.2	111	10.4	94 ± 16	3.4 ± 0.4	1.57 ± 0.05	-16%

Table 1 shows that for all samples the average of the nanocrystals size not greater than 5 nm in diameter, from which it follows that the optical properties of the films must be influenced by quantum confinement, which in turn will be influenced by the density of these nanocrystals and their distribution within the matrix of amorphous silicon [8].

As seen from the table, for both pressures is observed that  $D_R$  tends to increase with hydrogen dilution. In the system SiH<sub>2</sub>Cl<sub>2</sub> when SiH<sub>x</sub>Cl<sub>y</sub> species ( $x + y < 3$ ) hit the surface of growth, both the hydrogen and chlorine are preferentially extracted as HCl. Exothermic reaction of atomic hydrogen with chlorine emit a considerable amount of energy sufficient to promote the local crystallization [3]. So by increasing the hydrogen dilution, more nanocrystals are formed in the films of pm-Si:H with increasing size. While the increased pressure the mean free path of the gas species decreases, decreasing the extraction of hydrogen and chlorine, and exothermic reactions thereby increasing the local crystallization of the material.

### 3.2. CHEMICAL PROPERTIES.

#### 3.2.1. X-ray photoelectron spectroscopy, XPS.

Figure 1 shows the chemical composition profiles of all samples to different depths probed by sputtering the surface with argon ions for different erosion times in vacuum. The atomic percent corresponding to Cl, O and Si are reported, because hydrogen is not detectable by this technique.

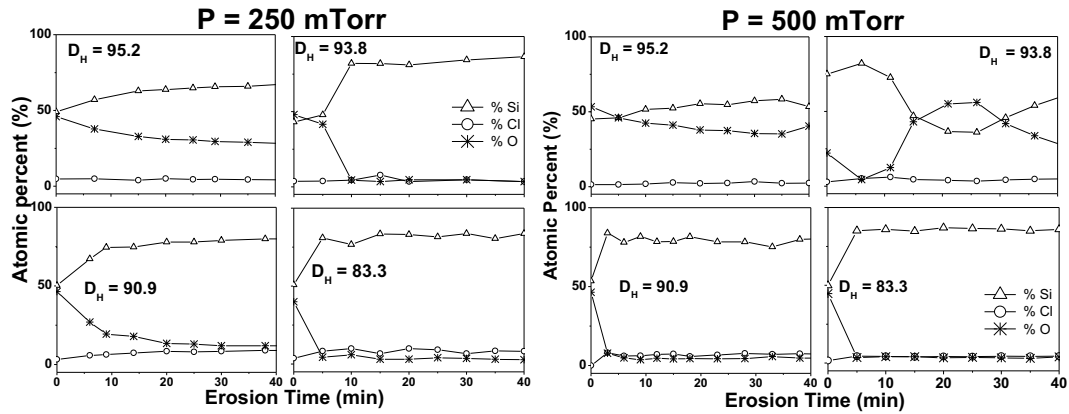


Fig. 1. Composition profiles of pm-Si:H thin films including atomic percents from Cl 2p, O 1s and Si 2p peaks for different argon ion erosion times.

Fig 1. Shows how the films are mainly composed by silicon (triangles). However, important concentrations of oxygen (asterisk) are detected in some samples. The amount of chlorine (circles) is always lower than 10%. It is possible to observe that in some cases Si and O concentrations changed with erosion time. In the film surface oxygen concentrations around 50% are detected in all samples. This value decreases to less than 15% with erosion time, except in some samples with elevated  $D_H$  where oxygen concentration remains above 25% for all erosion times. The appearance of O in some samples is the result of porous and less dense in the grain boundary regions, which facilitates absorption of oxygen on the surface of micro-voids, when the films are in ambient. Some studies have been noted that by introducing small amounts of oxygen introduced to the  $\mu$ -network further decreased the optical absorption and conductivity [14]; these effects are discussed below.

These results suggest that the films deposited at  $D_H$  of 83.3 and 90.9 have qualitatively better measure of the density and compact structure compare to films deposited at  $D_H$  of 93.8 and 95.2, for both pressure. The high  $D_H$  values of our films can attributed to a more porous structure, possibly caused by the nucleation of nano-sized crystallites in the amorphous network.

### 3.2.2. Fourier transform infrared spectroscopy, FTIR.

Figure 2 shows the spectra of FTIR transmission curves in the wave number range 550–800 and 1900–2400  $\text{cm}^{-1}$  for the most representative samples deposited at different  $D_H$  for pressures of 250 mTorr.

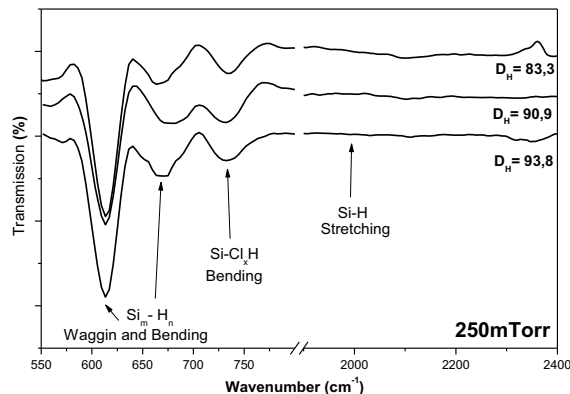


Fig 2. Infrared spectra of pm-Si:H films deposited at 250 mTorr showing the absorbance peaks, for three different hydrogen dilutions.

Fig. 2 exhibit that the Si-H stretching mode around 1900–2100  $\text{cm}^{-1}$  cannot be distinguished in our samples.

This band is generally associated to silicon hydrides incorporated into the amorphous matrix which are related with weak hydrogen bonds that are prone to generate light induced degradation of the material [4], [11], [15]. Instead, the  $\text{Si}_m\text{H}_n$  wagging mode around  $620\text{--}640\text{ cm}^{-1}$  and  $\text{SiCl}_x\text{H}$  bending mode at  $744\text{--}775\text{ cm}^{-1}$  is present in all cases [11] [16]. The  $\text{Si}_m\text{H}_n$  wagging mode has been correlated mainly with surface passivation of silicon nanocrystals in these type of pm-Si films [4], [10], [14]. Whereas  $\text{SiCl}_x\text{H}$  bending mode is associated to the small amount of incorporated chlorine in the films (less than 10 at.%, agree with the XPS analysis) [16], [17]. Based in results of XPS the FTIR transmission spectra should show signature of the Si–O peak near  $1000\text{--}1100\text{ cm}^{-1}$ , which also can't be distinguished.

From the perspective of application of these films as photovoltaic materials, having a high fraction crystalline in as grown films with low hydrides content in the amorphous matrix, is adequate for their utilization in silicon thin film solar cells.

### 3.3. OPTOELECTRONIC CHARACTERISTICS.

#### 3.3.1. Optical Band gap, $E_g^{op}$ .

Optical properties of our thin films were investigated from UV–VIS spectroscopy. Fig. 3 shows the variation of the effective optical band gap,  $E_g^{op}$  as a function of the structural properties through of  $D_R$  and  $X_C$ , for samples grown at 250 and 500 mTorr of pressure, respectively. The optical band gap energy  $E_g^{op}$  was obtained by the Tauc plot  $(\alpha h\nu)^{1/2}$  vs.  $(h\nu - E_g^{op})$  where  $\alpha$  is the absorbance,  $\nu$  is the frequency and  $h$  is the Planck constant. Tauc's plot is an effective method to determine the energy bandgap in amorphous thin film materials [18] [19].

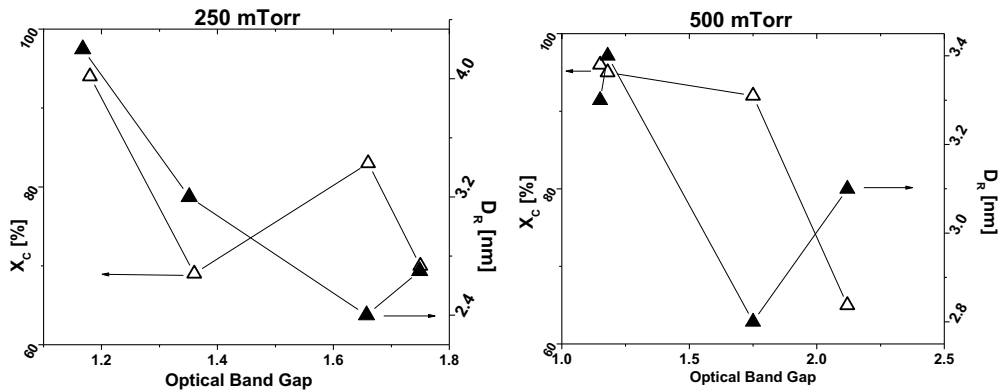


Fig. 3. crystalline volume fraction,  $X_C$  (open triangle) and mean grain size,  $D_R$  (solid triangle) as a function of Optical band Gap,  $E_g^{op}$ , to pressures of 250 and 500 mTorr.

We can see in fig. 3 is how  $E_g^{op}$  is modified by the structural parameters  $X_C$  and  $D_R$  and we found a tunable band gap in function of  $D_R$ . As seen from the figure, the  $E_g^{op}$  of films increases from 1.18 to 1.75 eV when  $D_R$  is decreased from 4.2 to 2.7 nm for samples grown at 250 mTorr, while for films 500mTorr it is difficult to comment this behavior due to the estimated values of  $D_R$  are almost a constant ( $\Delta D_R < 1\text{ nm}$ , see Table 1). However, it is too possible to note that  $E_g^{op}$  tends to decrease as  $X_C$  increase for both pressures. Accordingly, in the case of a mixed phase of crystalline and amorphous, i.e. nanocrystalline phase, the band gap should lie between amorphous and crystalline silicon. The typical value of the band gap of hydrogenated amorphous silicon (a-Si:H) is about 1.6 eV [19]. The higher band gap in pm-Si:H thin films in the present case may be due to the quantum size effect [8], [14], [19], [20]. So the behavior in  $E_g^{op}$  support the influence of quantum confinement as  $E_g^{op} \approx E_g + \frac{\hbar^2 \pi^2}{2\mu D_R^2}$  where  $E_g^{op}$  is the bulk material gap and  $\mu$  It is the reduced mass of electron-hole pair [8], [20]. Then  $E_g^{op}$  tends to decrease with the increase in  $D_R$  of embedded nanoclusters and randomly

distributed in the amorphous network of pm-Si:H thin films. One may argue that the increased band gap of the films is due to the presence of oxygen in these films. However the FTIR transmission of the films, taken immediately after the deposition, do not show the presence of Si–O bonds (near 1000–1100  $\text{cm}^{-1}$ ), though the feature appeared in some of the films when these are stored for a couple of week at room temperature.

### 3.3.1. Photoconductivity, $\sigma_p$ .

Photoconductivity measurement of the samples, using white light illumination of  $100\text{mW}/\text{cm}^2$ , during continuous light 250h were performed. We observe important behaviors in Photoconductivity for samples with high and low  $D_H$  and Pressure, as can be seen in fig 4. The results and  $D_R$  and  $X_C$  values obtained by Raman are mentioned in Fig. 4 and also in Tables 1.

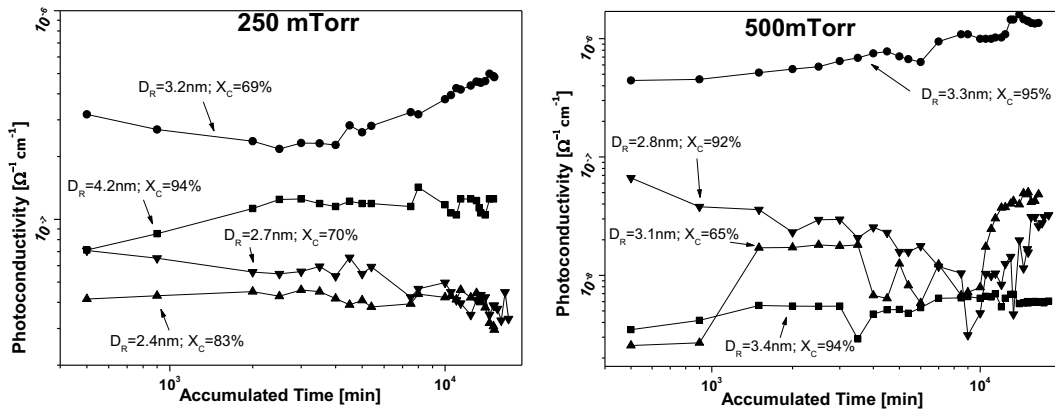


Fig. 4. Photoconductivity versus illumination time for pm-Si:H thin films

It is observed from Fig. 4 can not be distinguished stability in photoconductivity, instead we can see tendency to degrade over the time of light soaking in most films. We calculated different degradation rates of  $\sigma_p$  which are shown in Table 1 as  $(\sigma_{pi} - \sigma_{pf})/\sigma_{pi}$ , where  $\sigma_{pi}$  and  $\sigma_{pf}$  are inicial and final photoconductivity, respectively. If these values of degradation are negative then we call them improvement, so we could see improvement in the films whit high  $D_R$  and  $D_H$  for both pressures. This behavior could be due to improved pasivation process; sinse on the one hand, is closely related to the fact that the Si-O bond is stronger than the Si-Si bond and the Si-H bond. And the other, transport can be influenced by change in mobility due to the space charge between the crystalline and amorphous interfaces, by the incorporation of oxygen as a terminal bond.

## 4. Conclusion.

We have shown that optoelectronics characteristics of pm-Si:H thin films can be modulated by structural and chemical properties which depend of grown conditions is PECVD system using dichlorosilane. The chlorine chemistry introduced by the silicon precursor favors the formation of nanocrystalline inclusions. Raman measurements confirm that our films are nanocrystalline, with crystal average size on the range 2–3.5 nm. We found by XPS measurements, films deposited with high  $D_H$  present a considerable amount of oxidation evidence. Since on the other hand, From Fourier transform infrared spectroscopy analysis we notice that weak silicon hydride (Si-H) bonds were not detected while bonding configurations associated to the silicon nanocrystal surface ( $\text{Si}_m\text{H}_n$ ) were clearly observed. This result is largely related to possible photostability of our samples. By UV-Vis measurements we found a tunable band gap in function of  $D_R$ , with a behavior that support the influence of quantum confinement, while for the photoconductivity do not show stability in the samples, instead we obtained improvement of photoconductivity in the films whit high  $D_R$  and  $D_H$  for both pressures. Understanding structural and chemical properties of pm-Si:H thin films is key towards optimizing their electrical and optical properties for applications in solar cells.

## 5. Acknowledgements.

We acknowledge financial support for this work from CONACyT Mexico through postdoctoral scholarship CVU 165872. The authors are grateful to Dr. J.C. Alonso and Dr. A. Ortiz<sup>†</sup> for the use of laboratory facilities and Dr. A. Remolina for samples preparation.

## 6. References

- [1] H. Shirai, "Role of chlorine in the nanocrystalline silicon film formation by rf plasma-enhanced chemical vapor deposition of chlorinated materials," *Thin Solid Films*, vol. 457, no. 1, pp. 90–96, Jun. 2004.
- [2] R. Butté, S. Vignoli, M. Meaudre, R. Meaudre, O. Marty, L. Saviot, and P. Roca i Cabarrocas, "Structural, optical and electronic properties of hydrogenated polymorphous silicon films deposited at 150°C," *J. Non. Cryst. Solids*, vol. 266–269, pp. 263–268, May 2000.
- [3] C. Álvarez-Macias, J. Santoyo-Salazar, B. Monroy, M. García-Sánchez, M. Picquart, A. Ponce, G. Contreras-Puente, and G. Santana, "Estructura y morfología de películas de pm-Si: H crecidas por PECVD variando la dilución de diclorosilano con hidrógeno y la presión de trabajo," *Rev. Mex. física*, vol. 57, no. 3, pp. 224–231, 2011.
- [4] Álvarez-Macias, C., B.M. Monroy, L. Huertaa, M. Canseco-Martínez, M. Picquart, J. Santoyo-Salazar, M.F. García Sánchez, and G. Santana, "Chemical and structural properties of polymorphous silicon thin films grown from dichlorosilane," *Appl. Surf. Sci.*, vol. 285-B, pp. 431–439, 2013.
- [5] A. F. M. U and P. R. Cabarrocas, "Shedding light on the growth of amorphous , polymorphous , protocrystalline and microcrystalline silicon thin films," *Thin Solid Films*, pp. 161–164, 2001.
- [6] A. K. O. Odziej, "Staebler-Wronski effect in amorphous silicon and its alloys," *Sci. Technol.*, vol. 12, no. 1, pp. 21–32, 2004.
- [7] C. Álvarez-Macias, B. M. Monroy, L. Huerta, M. Picquart, and M. F. García, "Influence of light-soaking treatment on the optoelectronics properties of silicon polymorphous thin films to be used in solar cells .," in *Photovoltaic Specialists Conference (PVSC), 2013 IEEE 39th*, 2013, vol. 39th, pp. 0526 – 0529.
- [8] A. Remolina, B. M. Monroy, M. F. García-Sánchez, a Ponce, M. Bizarro, J. C. Alonso, a Ortiz, and G. Santana, "Polymorphous silicon thin films obtained by plasma-enhanced chemical vapor deposition using dichlorosilane as silicon precursor.," *Nanotechnology*, vol. 20, no. 24, p. 245604, Jun. 2009.
- [9] A. Ali, "Mechanisms of the growth of nanocrystalline Si:H films deposited by PECVD," *J. Non. Cryst. Solids*, vol. 352, no. 28–29, pp. 3126–3133, Aug. 2006.
- [10] S. Liu, X. Zeng, W. Peng, H. Xiao, W. Yao, X. Xie, C. Wang, and Z. Wang, "Improvement of amorphous silicon n-i-p solar cells by incorporating double-layer hydrogenated nanocrystalline silicon structure," *J. Non. Cryst. Solids*, vol. 357, no. 1, pp. 121–125, Jan. 2011.
- [11] L. Zhang, J. H. Gao, J. Q. Xiao, L. S. Wen, J. Gong, and C. Sun, "Low-temperature (120°C) growth of nanocrystalline silicon films prepared by plasma enhanced chemical vapor deposition from SiCl<sub>4</sub>/H<sub>2</sub> gases: Microstructure characterization," *Appl. Surf. Sci.*, vol. 258, no. 7, pp. 3221–3226, Jan. 2012.
- [12] C. Tu, T. Chang, P. Liu, C. Yang, and L. Feng, "Performance enhancement of excimer laser crystallized poly-Si thin film transistors with fluorine implantation technology," *Thin Solid Films*, 2007.

- [13] Y.-H. Chen, Y.-T. Liu, C.-F. Huang, J. C. Liu, and C. C. Lin, "Improved photovoltaic properties of amorphous silicon thin-film solar cells with an un-doped silicon oxide layer," *Mater. Sci. Semicond. Process.*, vol. 31, pp. 184–188, Mar. 2015.
- [14] P. Gogoi, H. S. Jha, and P. Agarwal, "High band gap nanocrystallite embedded amorphous silicon prepared by hotwire chemical vapour deposition," *Thin Solid Films*, vol. 518, no. 23, pp. 6818–6828, Sep. 2010.
- [15] B. Yan, L. Zhao, B. Zhao, J. Chen, G. Wang, H. Diao, Y. Mao, and W. Wang, "Hydrogenated amorphous silicon germanium alloy with enhanced photosensitivity prepared by plasma enhanced chemical vapor deposition at high temperature," *Vacuum*, vol. 89, pp. 43–46, 2013.
- [16] T. Ito, K. Hashimoto, and H. Shirai, "Surface Chemistry of Si:H:Cl Film Formation by RF Plasma-Enhanced Chemical Vapor Deposition of SiH<sub>2</sub>Cl<sub>2</sub> and SiCl<sub>4</sub>," *Jpn. J. Appl. Phys.*, vol. 42, no. Part 2, No. 10A, pp. L1119–L1122, Oct. 2003.
- [17] S. Jung, Y. Fujimura, T. Ito, and H. Shirai, "Chemistry of the chlorine-terminated surface for low-temperature growth of crystal silicon films by RF plasma-enhanced chemical vapor deposition," *Sol. Energy Mater.*, vol. 74, pp. 421–427, 2002.
- [18] L. Guo, J. Ding, J. Yang, G. Cheng, Z. Ling, and N. Yuan, "Effects of high hydrogen dilution ratio on optical properties of hydrogenated nanocrystalline silicon thin films," *Appl. Surf. Sci.*, vol. 257, no. 23, pp. 9840–9845, Sep. 2011.
- [19] V. S. Waman, M. M. Kamble, M. R. Pramod, S. P. Gore, a. M. Funde, R. R. Hawaldar, D. P. Amalnerkar, V. G. Sathe, S. W. Gosavi, and S. R. Jadhkar, "Influence of the deposition parameters on the microstructure and opto-electrical properties of hydrogenated nanocrystalline silicon films by HW-CVD," *J. Non. Cryst. Solids*, vol. 357, no. 21, pp. 3616–3622, Nov. 2011.
- [20] G. Santana, B. M. Monroy, a. Ortiz, L. Huerta, J. C. Alonso, J. Fandiño, J. Aguilar-Hernández, E. Hoyos, F. Cruz-Gandarilla, and G. Contreras-Puentes, "Influence of the surrounding host in obtaining tunable and strong visible photoluminescence from silicon nanoparticles," *Appl. Phys. Lett.*, vol. 88, no. 4, p. 041916, 2006.